A Miniaturized Microstrip Antenna for Ultra-wideband Applications

Nivedita Mishra[1], Saima Beg[2]
[1, 2]Department of Electronics and Communication Engineering, Integral University Lucknow, India - 226026.
Corresponding author: Nivedita Mishra (e-mail: nivimini01@gmail.com, saimabeg@iul.ac.in)

ABSTRACT In this paper, the authors present an ultra-wideband (UWB) planar antenna with defected ground structure (DGS) for various wireless applications. The operating frequency of the proposed geometry is in the range of 3.1 to 10.6 GHz. The proposed compact geometry antenna is applicable for the UWB applications. In order to optimize the dimensions of the antenna, a parametric analysis has been performed. The measured S_{11} magnitude is less than -10 dB over the band, and it has an impedance bandwidth of 10.60 GHz. The designed UWB antenna gives maximum radiation efficiency and gain of 96.5% and 3.30 dBi, respectively. Also, it gives good time-domain characteristics over the entire resonating band. The designed UWB antenna is simple geometry, and it is applicable for numerous wireless applications.

INDEX TERMS Microstrip Patch Antenna, Monopole, Ultra-wideband, Wireless Applications

I. INTRODUCTION

Recently, Ultra-wideband antennas (UWB) are playing a vital role in designing wireless communication frameworks, especially for the wireless local area (WLAN) and World interoperability for microwave access (WiMAX) network [1]. Microstrip patch antenna (MPA) is mainly used as a UWB antenna with its miniaturized size, multiband, and omni-directional patter [2] for these applications. MPA is also exceptionally well known because of its straightforwardness design and adaptability of enhancement to meet the antenna performance [3].

For better antenna design, a few strategies such as partial ground, increasing substrate thickness, and different slots consolidated on the antenna [4]. Utilizing the fractional ground plane, UWB transferable speed can be effectively acquired, and further, with various spaces, the band notch attributes can be handily gotten [5]. As of late, a few methods have been formed at UWB frequency with double band-notch attributes for various sorts of utilizations in [6]. The UWB antenna is implemented for dual-band rejection using the coplanar waveguide (CPW) feeding method in [7]. Two balanced spaces are added on the ground plane by planning a ring-opening on the transmitting patch to accomplish the primary band-notch. Nonetheless, just two frequency bands were engaged in [8-9]. The implemented antenna in [10] was persuaded by TL-MTM work and an L-formed space on the ground. In literature, many antennas are proposed, but the lack of compactness is the main problem in [11-13].

In [14], a smaller shape UWB monopole antenna is proposed for WLAN applications. A C-shaped slot has obtained the dual notch bands. It has accomplished a minor component of 34×30 mm^2 nearby with UWB transmission capacity for the upper WLAN band. A fascinating UWB antenna with a blend of U-shape stab on the patch and W-shape slots on the implemented ground was proposed in [15]. Hence, the developed radio wire has acquired 8.61 GHz data transmission alongside a double band-dismissal trademark for UWB applications. The antenna has disposed of the WiMAX and WLAN frequency band separately. A monopole antenna with the improvement for WLAN applications has been proposed in [16-17]. The fabricated antenna has a wide working data transmission of 3.1 - 11 GHz with satisfactory VSWR esteem (< 2) for the full transfer speed. The antenna has an area of 35×24 mm^2. In [18-22], a CPW-took care of material radio wire is presented for UWB application with the double band rejection for Bluetooth and WIMAX applications. The implemented design has a wide working transmission capacity of is 8.9 GHz capacities. The accomplished double bands are $2.3 - 2.5$ GHz and 3.3 - 3.7 GHz for Bluetooth and WIMAX applications. Two split ring resonator spaces have been planned on the radiating component to get double band rejection qualities. Notwithstanding, it has a wide area dimension of 43×40 mm^2. It is seen from the literature that the more significant part of the antenna has a somewhat enormous measurement that necessities to lessen by proposing an antenna for the application.

This paper proposes a triple-band microstrip patch antenna for WiMAX/LWLAN/UWLAN and downlink C-band sat beneficiary applications. A new plan of the UWB work has been proposed by embedding strips on wideband printed open space antenna by picking the legitimate boundaries of the strips to dismiss single, double band operation. Further, the proposed geometry is single layer and compact. The simulated and measured impedance bandwidth of 10.45 GHz and

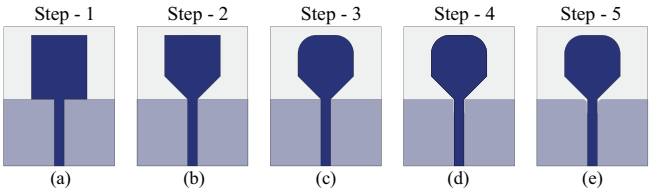

FIGURE 1: (a) - (e) Step -by- step formation of proposed single element.

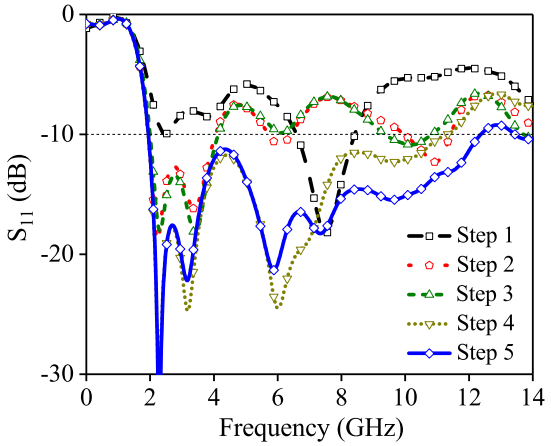

FIGURE 2: Intermediate steps effect on reflection coefficient.

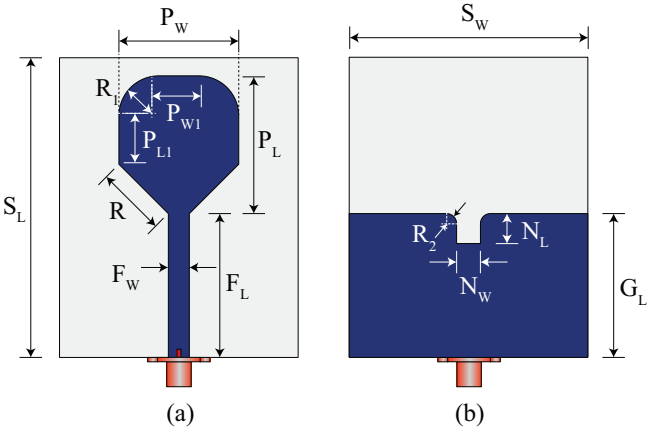

FIGURE 3: Proposed miniaturized single element: (a) Top-view. (b) Back-view.

TABLE 1: Detailed dimensions of proposed single element

Symbol	S_L	S_W	P_L	P_W	R
Value [mm]	50.00	40.00	23.00	20.00	11.66
Symbol	F_L	F_W	N_L	N_W	G_L
Value [mm]	24.00	3.50	5.00	4.00	24.00
Symbol	P_{L1}	P_{W1}	R_1	R_2	–
Value [mm]	8.10	6.68	6.66	1.66	–

10.60 GHz, respectively. The designed antenna has to gain variations from $1.1-3.3$ dBi over the entire resonating band. Further, it has a radiation efficiency variation of $87-96\%$. The simulated and measured results are almost matched. Also, the designed UWB antenna is compact and applicable for various observed bands such as World Interoperability for Microwave Access (WiMAX) - 3.3 to 3.6 GHz, Lower Wireless Local Area Network (LWLAN) - 5.15 to 5.35 GHz, Upper Wireless Local Area Network (UWLAN) - 5.75 to 5.85 GHz, and downlink C-Band sat receiver - 7.25 to 7.75 GHz.

The rest of the paper is organized as follows: The proposed geometry step formation, and a single element, are described in Section II. Then, the parametric analysis is performed in Section III. Next, the simulation and measurement results such as reflection coefficient, radiation patterns, gain, and time-domain analysis have been given in Section IV. Finally, Section V presents the conclusion of the proposed work.

II. PROPOSED ANTENNA DESIGN

This section presents the step-by-step formation of the proposed ultra-wideband microstrip patch antenna and its corresponding effect on the reflection coefficient. Also, the proposed single element realization, as well as optimized dimension, are discussed.

A. STEP FORMATION OF PROPOSED DESIGN

The step-by-step formation of the proposed antenna geometry is depicted in Fig. 1. First, the conventional square-shaped geometry with a half-ground plane is considered, and its corresponding reflection coefficient is plotted in Fig. 2. From Fig. 2, it can be seen that the designed conventional square geometry resonates at around 7 GHz with low impedance bandwidth. In step-2, the truncated corner has been introduced in a top patch with the same size ground plane, and corresponding S_{11} is depicted in Fig. 2. It can be seen that after introducing the truncated corner, the resonating frequency is shifted lower side. After introducing a truncated corner, the current path has been stretched which leads to electric travel for long distances. In step-3, the curve on the top patch is added, and it resonates at a lower band with good bandwidth. In step-4, the simple rectangular notch is added and its shown in Fig. 1(d). After adding a notch on the ground plane, the designed antenna resonates with a wideband. Finally, in step-5, the curve on the ground plane notch has been introduced and illustrated in Fig. 1(e). The corresponding S_{11} (Solid Blue Line) magnitude of the proposed design is given in Fig. 2. It can be seen that the designed antenna resonated in the UWB range (3.1 - 10.60 GHz). Inspired from results, the step 5 design is considered for UWB wireless applications.

B. SINGLE ELEMENT

The proposed design on step 5 is etched on top of the substrate material, shown in Fig. 3. The FR-4 substrate material has been utilized for the implemented antenna. The reason is that the FR-4 substrate material is easily available in the market as well as it is low-cost material. The overall substrate size is 40×50 mm^2. The defected ground surface (DGS) is employed to the proposed antenna instead of the full

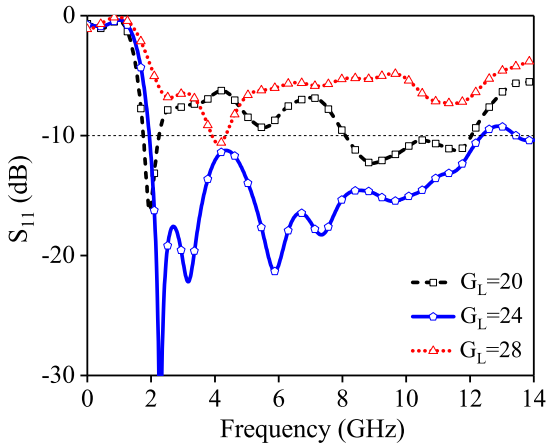

(a)

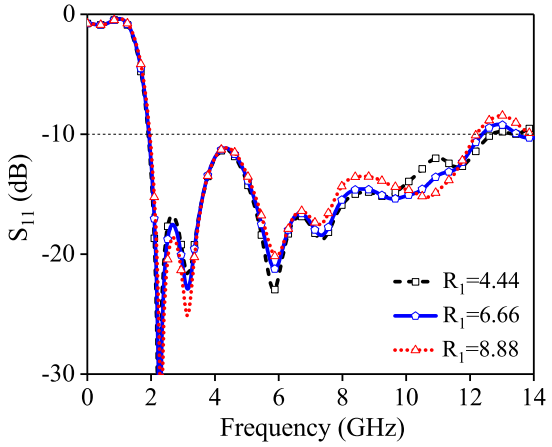

(b)

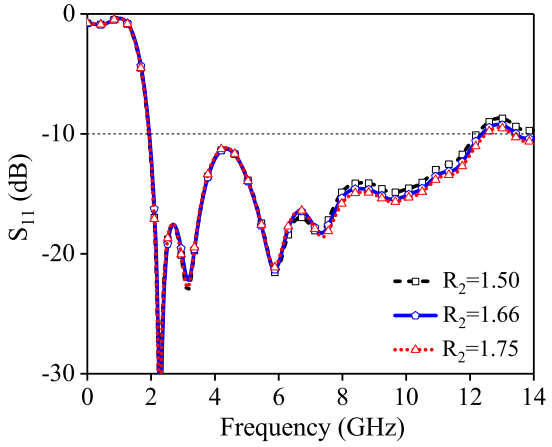

(c)

FIGURE 4: Effect on S_{11}: (a) Ground length G_L variation. (b) Top patch curve R_1 variation. (c) Ground notch curve R_2 variation.

ground structure to get high bandwidth with a better matching property. The proposed DGS in the antenna is a traditional rectangular shape attached to the substrate. An additional notch is taken in the middle of the DGS. The area of the notch is 4×3.34 mm^2. The radius of the curves on both sides of the notch is taken 1.66 mm. The top-view and bottom view of the proposed UWB antenna are illustrated in Fig. 3(a) and (b), respectively. Further, the detailed optimized dimension is given in Table 1. In the radiator, the patch is connected with a feed line to feed power in the patch. The 50Ω inset feed line is used to feed power in the patch. The dimension of the feed line is taken 3.50×24 mm^2. Both sides of the patch are cut with a 6.66 mm radius curve. The printed design of the proposed microstrip patch antenna can create an ultra-wide frequency band. UWB data transfer potency is accomplished by changing the radiuses of the curves in a patch and the size in DGS. The proposed antenna structure is easy to design for practical purposes, and it can provide an excellent stable impedance bandwidth in UWB operation. In designing the antenna, the lowest operating f_l is predicted, as in [20].

$$f_l = \frac{c}{4\sqrt{\varepsilon_{eff} \times \frac{L}{2}}} \tag{1}$$

$$\varepsilon_{eff} = \frac{\varepsilon_r + 1}{2} \tag{2}$$

Where c, ε_r, and ε_{eff} are the velocity of light, a dielectric constant, and effective dielectric constant of the substrate, respectively. As a result of this changing the length (L) of the patch antenna, the impedance matching property can be altered to the desired range. In this antenna, the length of an antenna is taken 23 mm to get better impedance matching.

III. PARAMETRIC ANALYSIS

At first, numerical simulation of the proposed UWB MPA is conducted in the CST software using the transient solver assessment and then experimentally verifying the simulated result. Then, a designed antenna is simulated from 0 GHz to 14 GHz to observe the reflection coefficient, voltage standing wave ratio (VSWR), radiation patterns, gain, and radiation efficiency. The comparative study for different sizes (G_L) of DGS, top patch curve (R_1), and ground notch (R_2) are also examined to observe the change of bandwidth using S_{11} magnitude.

The parametric analysis and effect on the S_{11} magnitude are illustrated in Fig. 4. The ground plane length (G_L) variation from 20 to 28 mm with a 4 mm gap and its effect on the reflection coefficient is presented in Fig. 4(a). It can be seen that for particular $G_L = 24$ mm, the proposed UWB gives good performance and achieve wideband as compared to other values. Similarly, the top patch notch (R_1) variations from 4.44 to 8.88 mm have been performed, and its effect on the reflection coefficient is depicted in Fig. 4(b). Similarly, the bottom notch (R_2) variations and effect on S_{11} magnitude is illustrated in Fig. 4(c). Thus, the UWB antenna gives wide bandwidth and good performance results for wireless applications for optimized and perfect value.

IV. SIMULATION AND MEASUREMENT RESULTS

The photograph of the manufactured model proposed UWB antenna is portrayed in Fig. 5. From Fig. 5, it can be seen

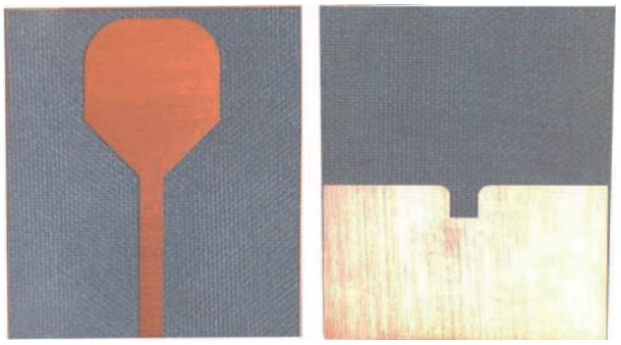

(a) (b)

FIGURE 5: Prototype of proposed single element: (a) Top-view. (b Back-view.

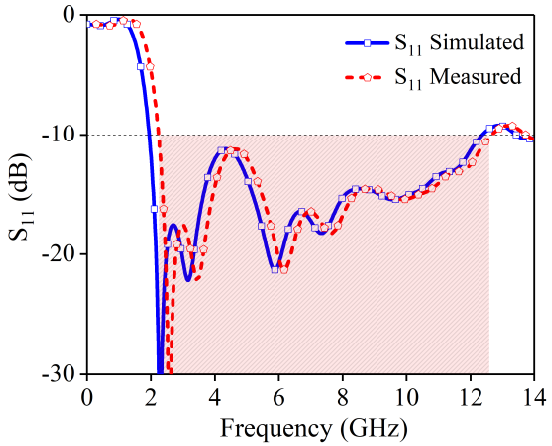

FIGURE 6: Simulated and measured reflection coefficient of the proposed single element.

that the proposed antenna is a compact and straightforward geometric configuration. Fig. 5(a) and (b) provide the top and back-view of the proposed geometry. The proposed antenna is fabricated and etched on top of the low-cost FR-4 material.

A. REFLECTION COEFFICIENT AND E-FIELD

The proposed UWB designed antenna simulated and measured S_{11} magnitude comparison is depicted in Fig. 6. It is seen from Fig. 6 that the measured and simulated S_{11} magnitude is approximately similar. The simulated antenna resonates from $1.93-12.38$ GHz while the measured reading is obtained at $2.1-12.70$ GHz. Also, the sharp S_{11} notch of -39.66 dB at 2.26 GHz in simulation and -42 dB at 2.50 GHz in measurement. Further, the simulated impedance bandwidth from CST software is 10.45 GHz, and the resultant impedance bandwidth from the prototype antenna is 10.60 GHz. Besides, the return loss of the measurement section is lower compared to the simulated section. Also, the resultant VSWR is fewer than 2 between 1.93 to 12.38 GHz frequency ranges. With the goal that reception apparatus coordinate thought about generally excellent.

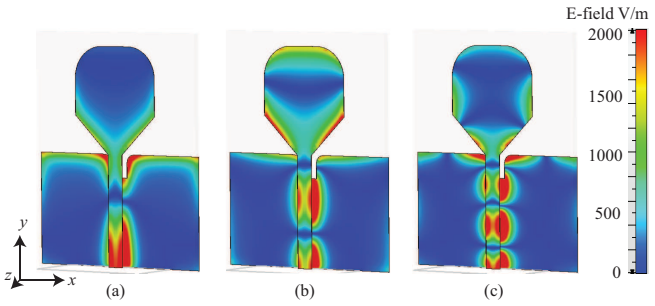

FIGURE 7: E-field distribution at: (a) 3 GHz. (b) 6 GHz. (c) 10 GHz.

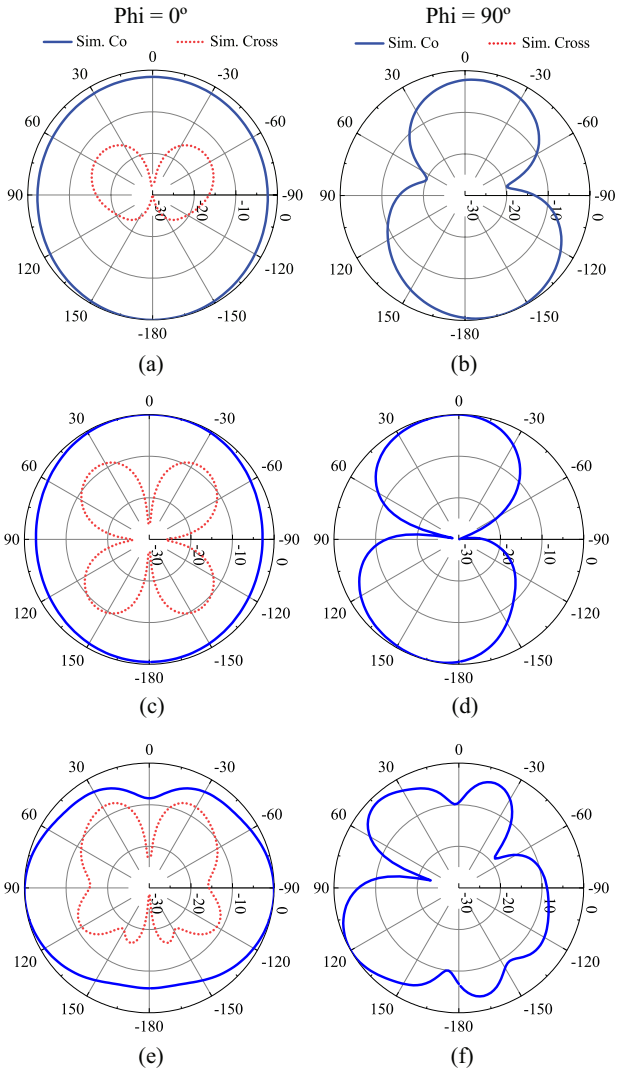

FIGURE 8: 2D radiation patterns of phi=0° and 90° planes at: (a)-(b) 3 GHz. (c)-(d) 6 GHz. (e)-(f) 10 GHz.

The E-field distribution at 3, 6, and 10 GHz frequencies are given in Fig. 7. Fig. 7(a) shows that at 3 GHz frequency, the highest E-field at the bottom side notches, which indicates the lower resonating notch is achieved due to the back notch. Similarly, for 6 GHz and 10 GHz, the designed patch

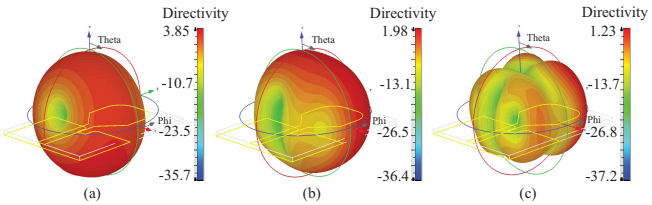

FIGURE 9: 3D radiation patterns at: (a) 3 GHz. (b) 6 GHz. (c) 10 GHz.

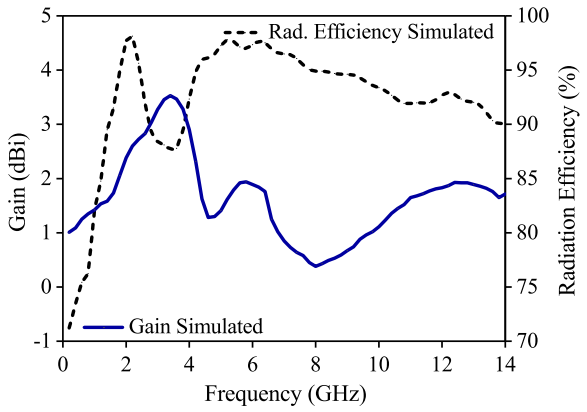

FIGURE 10: Simulated gain and radiation efficiency of proposed single element.

truncated sides and R_1 curve are responsible for the middle and higher bands, respectively. The most extreme E-field is noticed in the upper and lower layers of the patch. The proposed antenna gives good resonance at 6 GHz, as shown in Fig. 6. Also, the same can be seen in Fig. 7 which is electric field distribution where the more electric field is distributed at the edges of the radiating patch.

B. RADIATION PATTERNS

In Fig. 8, the polar plot for the far-field directivity is given. These are simulated at 3, 6, and 10 GHz at both E-plane ($\phi = 0°$) and H-plane ($\phi = 90°$). It is observed that the side lobe of the E-plane reduced with increasing frequency. As observed, the E-plane is not similar in shape as the frequency increases. The same case is also for H-plane. Overall the radiation pattern reflects the omni-directional and bi-directional for H-plane and E-plane by taking the characteristics of monopole antenna. So that, it can be seen that the primary beam tilts at upper recurrence. The sidelobe level is also changed in the antenna radiation with increasing frequency. The simulated gain of the proposed UWB antenna at 3, 6, and 10 GHz is 3.30, 1.86, and 1.10 dBi, respectively. The proposed antenna can provide enough gain for the WiMAX/LWLAN/ UWLAN, and downlink C-band sat receiver.

The output of the 3D radiation pattern is given in Fig. 9. The 3D radiation pattern is simulated at 3, 6, and 10 GHz to observe the change of directivity over the broadband. The radiation pattern of the antenna, without a doubt, emanates from the entire worked frequency range. The simulated directivity is 3.85 dBi at 3 GHz frequency. At 6 and 10 GHz, the directivity gain reduced slightly. The antenna provides enough directivity gain for the applications such as WIMAX, LWLAN, UWLAN, and downlink C-SAT receiver. Directivity depicted by the simulated UWB MPA is shown as a good possibility for this application.

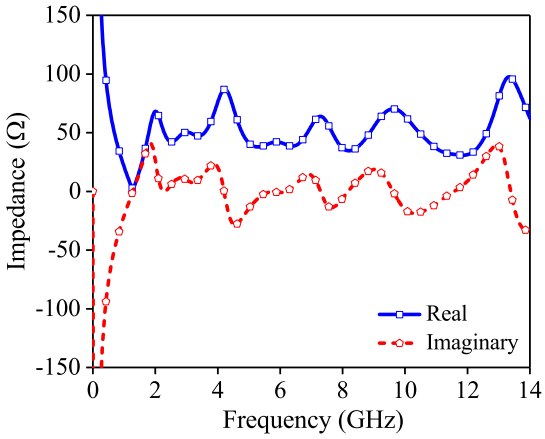

FIGURE 11: Proposed UWB antenna impedance.

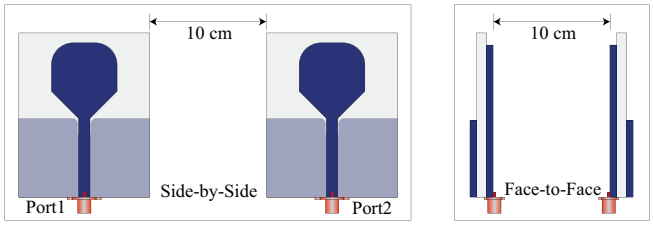

FIGURE 12: The time-domain characteristics setup in CST: (a) Side-by-Side. (b) Face-to-Face.

C. GAIN AND RADIATION EFFICIENCY

The simulated gain and radiation efficiency plot of the designed UWB antenna is given in Fig. 10. From Fig. 10, it can be found that the designed UWB gives a gain of 0.5 - 3.30 dBi variations over the resonating band. The maximum gain of 3.30 dBi is achieved at 3.50 GHz. Further, the radiation efficiency analysis results are illustrated in Fig. 10. The radiation efficiency of the proposed UWB antenna varies from $87 - 96\%$. The maximum radiation efficiency of 96.5% has been achieved at 5 GHz.

The impedance variations over the resonating band plot are illustrated in Fig. 11. From Fig. 11, it can be noted that the antenna has an almost constant impedance of 50Ω over the resonating band. However, the impedance varies between $40 - 60\Omega$ over the resonating band. Further, it can be seen that the impedance is not matched at lower 1 GHz and higher 14 GHz, which is due to the current being interrupted at a particular resonating frequency.

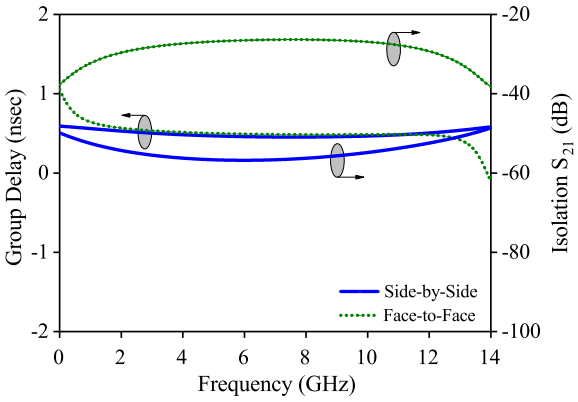

FIGURE 13: Proposed single element group delay and isolation

D. TIME-DOMAIN ANALYSIS

The time-domain analysis of the proposed UWB antenna in side-by-side (SS) and face-to-face (FF) conditions has been performed in the CST simulation environment. For both conditions, the group delay and phase response performance of the UWB antenna is performed. The experimental setup in face-to-face and side-by-side conditions at a distance of 10 cm is illustrated in Fig. 12. The UWB proposed antenna setup for both conditions is shown in Fig. 12(a), and (b), respectively, and both antennas work as transceivers. The group delay is the ratio of the negative rate of change of the transfer function to frequency. The mathematical formula is given below [23]:

$$\tau_g(\omega) = -\frac{d\phi(f)}{2\pi df} \tag{3}$$

Where ϕ is the phase response of the received signal, and the group delay versus frequency plot of the proposed UWB antenna is depicted in Fig. 13. From Fig. 13, it can be observed that the designed antenna has a group delay variation in the side-by-side condition is less than 0.60 nsec, and in the face-to-face condition, the variation is 0.75 nsec. The transfer function of the UWB antenna is given as [23]:

$$H(\omega) = \sqrt{\frac{2\pi c_0 D S_{21}(\omega) e^{\frac{j\omega D}{c_0}}}{j\omega}} \tag{4}$$

Here, D is the distance between the antenna, and the coupling between two ports can be identified using the isolation parameter. The isolation defined the ratio of power incident to the power delivered to another port. The isolation parameter (S_{21}) of the proposed geometry is given in Fig. 13. It can be noted that the designed geometry gives good isolation in both conditions, which is greater than -20 dB. Thus, the designed UWB antenna gives good time-domain characteristics over the entire resonating band and gives suitable performance parameters over the resonating band. Therefore, the proposed geometry is applicable for UWB wireless applications.

V. CONCLUSION

A microstrip antenna is designed with DGS for the UWB frequency range. The antenna size is a small, easy fabrication and provides the operation band of frequency over $3.1 - 10.6$ GHz. The measured impedance bandwidth of the proposed geometry is $2.1 - 12.70$ GHz. The designed prototype antenna performance is close to the simulation part from CST. The VSWR is also in the acceptable range. The radiation characteristics also provide some excellent properties. The measured maximum gain of the proposed geometry is 3.30 dBi at 3.50 GHz. Also, the radiation efficiency variations from $87 - 96\%$ over the resonating band. The operating far-field directivity is also very good for the application in WIMAX/LWLAN/ UWLAN, and downlink C-band sat receiver. Also, it gives good time-domain characteristics performance over the resonating band. Moreover, the experimental results matched well with the numerical antenna characteristics. Overall, the proposed antenna provides much better performance regarding the UWB application.

REFERENCES

[1] S. H. Hwang, J. I. Moon, W. I. Kwak, and S. O. Park, "Printed compact dual band antenna for 2.4 and 5 GHz ISM band applications," Electronics Letters, vol. 40, no. 25, pp. 1568–1569, 2004. doi:10.1049/el:20046579

[2] Y. C. Lin, and K. J. Hung, "Design of dual-band slot antenna with double T-match stubs," Electronics Letters, vol. 42, no. 8, pp. 438–439, 2006. doi:10.1049/el:20060009

[3] W. C. Liu, and H. J. Liu, "Compact triple-band slotted monopole antenna with asymmetrical CPW grounds," Electronics Letters, vol. 42, no. 15, pp. 840–842, 2006. doi:10.1049/el:20061119

[4] D. G. Patanvariya, and A. Chatterjee, "High gain and low cross-polarized printed array of Baravelle's spiral antennas for ku-band application," AEU-International Journal of Electronics and Communications, vol. 132, p.153634, 2021. doi:10.1016/j.aeue.2021.153634

[5] A. P. Zhao, and J. Rahola, "Quarter-wavelength wideband slot antenna for 3-5 GHz mobile applications," IEEE Antennas and Wireless Propagation Letters, vol. 4, pp. 421–424, 2005. doi:10.1109/LAWP.2005.859382

[6] N. Behdad, and K. Sarabandi, "Bandwidth enhancement and further size reduction of a class of miniaturized slot antennas," IEEE Transactions on Antennas and Propagation, vol. 52, no. 8, pp. 1928–1935, 2004. doi:10.1109/TAP.2004.832330

[7] J. Y. Li, and Y. B. Gan, "Multi-band characteristic of open sleeve antenna," Progress In Electromagnetics Research, vol. 58, pp. 135–148, 2006. doi:10.2528/PIER05090301

[8] Y. Song, Y. C. Jiao, G. Zhao, and F. S. Zhang, "Multiband CPW-fed triangle-shaped monopole antenna for wireless applications," Progress In Electromagnetics Research, vol. 70, pp. 329–336, 2007. doi:10.2528/PIER07020201

[9] J. Y. Sze, C. I. G. Hsu, and S. C. Hsu, "Design of a compact dual-band annular-ring slot antenna," IEEE Antennas and Wireless Propagation Letters, vol. 6, pp. 423–426, 2007. doi:10.1109/LAWP.2007.902053

[10] I. Barraj, H. Trabelsi, G. Bouzid, and M. Masmoudi, "Modeling, Design and Simulation of Low Complexity IR-UWB Transceiver for Medical Monitoring Applications," International Review on Modelling and Simulations (IREMOS), vol. 7, no. 2, pp. 331–340, 2014.

[11] C. C. Lin, P. Jin, and R. W. Ziolkowski, "Single, dual and tri-band-notched ultrawideband (UWB) antennas using capacitively loaded loop (CLL) resonators," IEEE Transactions on Antennas and Propagation, vol. 60, no. 1, pp. 102–109, 2011. doi:10.1109/TAP.2011.2167947

[12] J. A. Zubairi, Application of High Modern Performance Networks, Bentham eBooks, pp. 99–101, 2009.

[13] G. Manzi, M. Feliziani, P. A. Beeckman, and N. van Dijk, "Coexistence between ultra-wideband radio and narrow-band wireless LAN communication systems—part II: EMI evaluation," IEEE Transactions on Electromagnetic Compatibility, vol. 51, no. 2, pp. 382–390, 2009. doi:10.1109/TEMC.2008.2007648

[14] A. B. Lavanya, “Effects of electromagnetic radiation on biological systems: A short review of case studies," 8th International Conference on Electromagnetic Interference and Compatibility, pp. 87–90, 2003. doi:10.1109/ICEMIC.2003.237842

[15] Y. P. Shkolnikov, and W. H. Bailey, “Electromagnetic interference and exposure from household wireless networks," IEEE Symposium on Product Compliance Engineering Proceedings, pp. 1–5, 2011. doi:10.1109/PSES.2011.6088244

[16] Q. D. Ho, T. N. Tran, and T. Le-Ngoc, “Electromagnetic-interference-aware adaptive routing for wireless communication networks deployed in heath care institutions," 24th Canadian Conference on Electrical and Computer Engineering (CCECE), pp. 787–790, 2011. doi:10.1109/CCECE.2011.6030563

[17] C. K. Tang, K. H. Chan, L. C. Fung, and S. W. Leung, “Electromagnetic interference immunity testing of medical equipment to second-and third-generation mobile phones," IEEE Transactions on electromagnetic compatibility, vol. 51, no. 3, pp. 659–664, 2009. doi:10.1109/TEMC.2009.2021524

[18] S. Loyka, “Electromagnetic interference in wireless communications: behavioral-level simulation approach," IEEE 60th Vehicular Technology Conference VTC2004-Fall, no. 6, pp. 3945–3949, 2004. doi:10.1109/VETECF.2004.1404817

[19] D. H. Lee, H. Y. Yang, and Y. K. Cho, “Design and analysis of tapered slot antenna with 3.5/5.5 GHz band-notched characteristics," Progress In Electromagnetics Research B, vol. 56, pp. 347–363, 2013. doi:10.2528/PIERB13092702

[20] X. Q. Qi, H. C. Yang, D. Liu, and Y. Li, “Dual and tri-band-notched ultra-wideband (UWB) antennas using compact composite resonators," Progress in Electromagnetics Research Letters, vol. 42, pp. 177–185, 2013. doi:10.2528/PIERL13072303

[21] F. Xu, Z. X. Wang, X. Chen, and X. A. Wang, “Dual band-notched UWB antenna based on spiral electromagnetic-bandgap structure," Progress In Electromagnetics Research B, vol. 39, pp. 393–409, 2012. doi:10.2528/PIERB12021607

[22] T. G. Ma, and S. J. Wu, “Ultra wideband band-notched folded strip monopole antenna," IEEE Transactions on Antennas and Propagation, vol. 55, no. 9, pp. 2473–2479, 2007. doi:10.1109/TAP.2007.904137

[23] D. G. Patanvariya, and A. Chatterjee, “A Compact Bow-tie Shaped Wide-band Microstrip Patch Antenna for Future 5G Communication Networks," Radioengineering, vol. 30, no. 1, pp. 40–47, 2021. doi:10.13164/re.2021.0040